Deutsche Forschungsgemeinschaft
Priority Programme 1962

The Combination of POD Model Reduction with Adaptive Finite Element Methods in the Context of Phase Field Models

Carmen Gräßle, Michael Hinze

SPP 1962 | Non-smooth and Complementarity-based Distributed Parameter Systems: Simulation and Hierarchical Optimization

Preprint Number SPP1962-061

received on June 19, 2018

Edited by
SPP1962 at Weierstrass Institute for Applied Analysis and Stochastics (WIAS)
Leibniz Institute in the Forschungsverbund Berlin e.V.
Mohrenstraße 39, 10117 Berlin, Germany
E-Mail: spp1962@wias-berlin.de

World Wide Web: http://spp1962.wias-berlin.de/

PAMM · Proc. Appl. Math. Mech. **17**, 47 – 50 (2017) / **DOI** 10.1002/pamm.201710014

The combination of POD model reduction with adaptive finite element methods in the context of phase field models

Carmen Gräßle[1,*] and **Michael Hinze**[1,**]

[1] Universität Hamburg, Bundesstr. 55, 20146 Hamburg, Germany

In the present paper we derive a reduced order model utilizing proper orthogonal decomposition (POD-ROM), for which we utilize adaptively obtained spatial snapshots. In a fully discrete setting this contains the challenge that the snapshots are vectors of different lengths. In order to handle this issue, we interprete the snapshots as elements of a common Hilbert space and consider the POD method from an infinite-dimensional perspective. Thus, the inner product of pairs of snapshots can be computed explicitely, which enables us to build the reduced order model. This approach is applied to a phase field model which is described by a Cahn-Hilliard equation. In the numerical examples we illustrate our appoach and compare a nonsmooth with a smooth free energy concerning the influence on the quality of the solution to the ROM.

1 Introduction

For many problem settings, model order reduction utilizing proper orthogonal decomposition (POD-MOR) is known to be a powerful tool in order to reduce numerical effort by replacing large scale systems by low dimensional approximations. The POD method is based on a Galerkin ansatz, in which the ansatz functions (POD modes) contain information about the underlying dynamical system. According to snapshot based POD in [15], this system information is obtained from snapshots of the solution trajectory, which are generated in a simulation. In many pratical applications, spatially adaptive concepts are unavoidable in order to make simulations implementable. For example, in the context of phase field models, the interface formation and evolution can be described utilizing a diffuse interface approach. Many degrees of freedom are needed in order to well resemble the phase transitions, whereas in the pure phases a little number of degrees of freedom suffice. Even with the use of spatial adaptivity, numerical simulations and especially optimization can still be computationally expensive. This is why we apply POD model order reduction with the aim to speed up the computations. However, the combination of spatial adaptively generated snapshots with POD reduced order modeling contains the challenge that in a fully discrete setting the snapshots are vectors of different lengths due to the different spatial resolutions at each time instance. In order to deal with this issue, several ideas have been proposed. For example, in [8], a fixed reference mesh is utilized, onto which the h-adaptive snapshots are interpolated. Moreover, in [14] an interpolation approach is outlined, where given snapshots are interpolated by piecewise polynomials. Recently, the combination of POD model reduction with adaptive finite element snapshots is realized in [16] by constructing common finite element spaces. Two options are considered: either all snapshots are expressed in terms of a common finite element basis or pairs of snapshots are expressed in terms of a common finite element basis of these pairs. Finally, in [9], we derive a POD reduced order model for a general parabolic evolution equation utilizing arbitrary finite element discretizations. In this work, our focus lies on the POD model model order reduction for the Cahn-Hilliard equation which can be set up explicitely for arbitrary finite element discretizations.

2 The Cahn-Hilliard system

A common mathematical model to describe phase field systems utilizing a diffuse interface approach is the Cahn-Hilliard system. It was proposed in [5] as a model for phase separation in binary alloys. For a given a mixture of two components A and B, also referred to as phases, a phase field variable c is introduced in order to characterize the phase structures. In the regions of pure A-phase it is $c \equiv -1$ and in the pure B-phase it is $c \equiv +1$. The interfacial region is described by $c \in (-1, 1)$ and its thickness is finite and of order $\mathcal{O}(\varepsilon)$ with $0 < \varepsilon \ll 1$. Let $\Omega \subset \mathbb{R}^{\mathtt{d}}, \mathtt{d} \in \{2, 3\}$, denote a bounded open domain with Lipschitz continuous boundary $\partial\Omega$ and let $T > 0$ be a fixed end time. Introducing the chemical potential w, the Cahn-Hilliard equations can be formulated in a coupled system for the phase field c and the chemical potential w:

$$c_t(t, \boldsymbol{x}) + v(t, \boldsymbol{x}) \cdot \nabla c(t, \boldsymbol{x}) = m\Delta w(t, \boldsymbol{x}) \qquad \text{in } (0, T) \times \Omega, \tag{1a}$$

$$w(t, \boldsymbol{x}) = -\sigma\varepsilon\Delta c(t, \boldsymbol{x}) + \frac{\sigma}{\varepsilon} W'(c(t, \boldsymbol{x})) \qquad \text{in } (0, T) \times \Omega, \tag{1b}$$

* Corresponding author: e-mail carmen.graessle@uni-hamburg.de
** e-mail michael.hinze@uni-hamburg.de

with homogeneous Neumann boundary conditions $\nabla c(t,\boldsymbol{x})\cdot\nu_\Omega = \nabla w(t,\boldsymbol{x})\cdot\nu_\Omega = 0$ on $(0,T)\times\partial\Omega$ and the initial condition $c(0,\boldsymbol{x}) = c_0(\boldsymbol{x})$ in Ω. By ν_Ω we denote the outward normal on $\partial\Omega$, $m \geq 0$ is a constant mobility and $\sigma > 0$ denotes the surface tension. The convective term $v\cdot\nabla c$ describes the transport of the phase field with velocity v. Note that the transport term represents the coupling to the Navier-Stokes equations in the context of multiphase flow, see e.g. [10] and [2].

The free energy function $W(c)$ is of double-well type. A typical choice for W is the polynomial free energy function

$$W^p(c) = (1-c^2)^2/4, \tag{2}$$

which has exactly two minimal points at $c = \pm 1$, i.e. at the energetically favorable state. However, W^p allows c to have values $|c| > 1$ which are not meaningful from a physical perspective. Another choice for W is the relaxed double-obstacle free energy

$$W_s^{\text{rel}}(c) = \frac{1}{2}(1-c^2) + \frac{s}{2}(\max(c-1,0)^2 + \min(c+1,0)^2), \tag{3}$$

with relaxation parameter $s \gg 0$, which is introduced in [11] as the Moreau-Yosida relaxation of the double-obstacle free energy

$$W^\infty(c) = \begin{cases} \frac{1}{2}(1-c^2), & \text{if } c\in[-1,1], \\ +\infty, & \text{else.} \end{cases} \tag{4}$$

The double-obstacle free energy enforces $|c| \leq 1$. For more details on the choices for W we refer to [1] and [4], for example. Concerning existence, uniqueness and regularity of a solution to (1), we refer to e.g. [4].

3 POD reduced order modeling utilizing snapshots with arbitrary finite element discretizations

POD method in real Hilbert spaces. The objective of this work is to derive a POD-ROM for the Cahn-Hilliard system (1) which can be set up explicitely for spatially adaptive snapshots. For this reason, we consider the snapshots as elements of a common Hilbert space and apply the POD method in an infinite-dimensional setting. For further details about the POD method in Hilbert spaces, we refer to e.g. [13]. Here, we recall the main aspects.

Let $(V,\langle\cdot,\cdot\rangle_V)$ and $(H,\langle\cdot,\cdot\rangle_H)$ be real separable Hilbert spaces such that there exists a dense and continuous embedding $V \hookrightarrow H$. Assume, we are given snapshots $y^0\in V^0,\dots,y^n\in V^n$ belonging to different conformal subspaces $V^0,\dots,V^n \subset V \subset X$ with $X = V$ or $X = H$. By construction we have $\mathcal{V} = \text{span}\{y^j\}_{j=0}^n \subset V \subset X$. The key idea of the POD method in Hilbert spaces is to describe the space $\mathcal{V}$ by means of a few orthonormal functions $\{\psi_i\}_{i=1}^\ell \subset X$ with $\ell \leq d := \dim\mathcal{V}$ in the following sense:

$$\min_{\psi_1,\dots,\psi_\ell\in X} \sum_{j=0}^n \alpha_j \left\| y^j - \sum_{i=1}^\ell \langle y^j,\psi_i\rangle_X\ \psi_i \right\|_X^2 \quad \text{s.t. } \langle\psi_i,\psi_j\rangle_X = \delta_{ij} \quad \text{for } 1\leq i,j\leq\ell, \tag{5}$$

with $\{\alpha_j\}_{j=0}^n$ denoting nonnegative weights. A solution to (5) is called rank-ℓ POD basis. We introduce the linear bounded operator

$$\mathcal{Y}:\mathbb{R}^{n+1}\to X, \quad \mathcal{Y}\phi = \sum_{j=0}^n \sqrt{\alpha_j}\phi_j y^j \quad \text{for } \phi=(\phi_0,\dots,\phi_n)\in\mathbb{R}^{n+1} \tag{6}$$

and its Hilbert space adjoint

$$\mathcal{Y}^\star : X\to\mathbb{R}^{n+1}, \quad \mathcal{Y}^\star\psi = \left(\langle\psi,\sqrt{\alpha_0}y^0\rangle_X,\dots,\langle\psi,\sqrt{\alpha_n}y^n\rangle_X\right)^T \quad \text{for } \psi\in X. \tag{7}$$

Following the so-called *method of snapshots*, we consider the matrix

$$\mathcal{K} := \mathcal{Y}^\star\mathcal{Y}\in\mathbb{R}^{(n+1)\times(n+1)}, \quad \mathcal{K}_{ij} = \sqrt{\alpha_i}\sqrt{\alpha_j}\langle y^i,y^j\rangle_X \ \text{ for } i,j=0,\dots,n. \tag{8}$$

It is important to emphasize that each inner product of two snapshots from different finite element spaces can be computed explicitely, because they all live in a common Hilbert space. Moreover, the matrix dimension of $\mathcal{K}$ only depends on the number of utilized snapshots. Hence, $\mathcal{K}$ can be set up explicitely. Since $\mathcal{K}$ is symmetric and thus positive semi-definite, it follows that for the eigenvalue problem $\mathcal{K}\phi_i = \lambda_i\phi_i$, there exist $(n+1)$ nonnegative eigenvalues $\lambda_1\geq\dots\geq\lambda_d>0$ and $\lambda_i = 0$ for $i>d$ and corresponding eigenvectors $\phi_i\in\mathbb{R}^{n+1},\ 0\leq i\leq n$, which can be chosen pairwise orthonormal. Thus, the eigenvectors $\{\phi_i\}_{i=0}^n$ are the right singular vectors of $\mathcal{Y}$ and contain the space independent time information. It can be shown that a POD basis is given by

$$\psi_i = \frac{1}{\sqrt{\lambda_i}}\mathcal{Y}\phi_i \quad \text{for } 1\leq i\leq\ell. \tag{9}$$

POD reduced order modeling. We stay in the infinite-dimensional setting and derive the POD reduced order model for (1) utilizing the method of snapshots (8). For both the phase field c and the chemical potential w we make an individual POD Galerkin ansatz

$$c^\ell(t) = \sum_{i=1}^{\ell^c} \eta_i^c(t)\psi_i^c, \quad w^\ell(t) = \sum_{i=1}^{\ell^w} \eta_i^w(t)\psi_i^w \quad \text{for all } t \in [0,T]. \tag{10}$$

Inserting (10) into (1) and choosing $X_c^{\ell^c} = \text{span}\{\psi_1^c, \dots, \psi_{\ell^c}^c\} \subset X$ as test space for (1b) and $X_w^{\ell^w} = \text{span}\{\psi_1^w, \dots, \psi_{\ell^w}^w\} \subset X$ as test space for (1a) leads to the system

$$\left\{ \begin{array}{rcll} \frac{d}{dt}\langle c^\ell(t), \psi^w\rangle_H + \langle v\cdot\nabla c^\ell(t), \psi^w\rangle_H + m\langle \nabla w^\ell(t), \nabla\psi^w\rangle_H &=& 0 & \forall \psi^w \in X_w^{\ell^w}, \\ -\langle w^\ell(t), \psi^c\rangle_H + \sigma\varepsilon\langle \nabla c^\ell(t), \nabla\psi^c\rangle_H + \frac{\sigma}{\varepsilon}\langle W'(c^\ell(t)), \psi^c\rangle_{V',V} &=& 0 & \forall \psi^c \in X_c^{\ell^c}. \end{array} \right. \tag{11}$$

Since we want to construct a POD-ROM for arbitrary finite element discretizations, we rewrite (11) using the identity (9):

$$\left\{ \begin{array}{rcl} D^w(\Phi^w)^T\mathcal{K}_c^w\Phi^c D^c\dot\eta^c(t) + D^w(\Phi^w)^T\mathcal{T}\Phi^c D^c\eta^c(t) + mD^w(\Phi^w)^T\mathcal{A}_w^w\Phi^w D^w\eta^w(t) &=& 0, \\ -D^c(\Phi^c)^T\mathcal{K}_w^c\Phi^w D^w\eta^w(t) + \sigma\varepsilon D^c(\Phi^c)^T\mathcal{A}_c^c D^c\eta^c(t) + \frac{\sigma}{\varepsilon}\mathcal{N}(\eta^c(t)) &=& 0, \end{array} \right. \tag{12}$$

for $t \in (0,T]$ and $D^c(\Phi^c)^T\mathcal{K}_c^c\Phi^c D^c\eta^c(0) = D^c\bar\eta_0$, where $(\bar\eta_0)_i = \langle \mathcal{Y}_c^\star c_0, \phi_i^c\rangle_{\mathbb{R}^{n+1}}$ for $i = 1,\dots,\ell$. We use the following notation: $\eta^c = (\eta_1^c,\dots,\eta_{\ell^c}^c)^T \in \mathbb{R}^{\ell^c}$, $\eta^w = (\eta_1^w,\dots,\eta_{\ell^w}^w)^T \in \mathbb{R}^{\ell^w}$, $D^c = \text{diag}(1/\sqrt{\lambda_1^c},\dots,1/\sqrt{\lambda_{\ell_c}^c}) \in \mathbb{R}^{\ell^c\times\ell^c}$, $D^w = \text{diag}(1/\sqrt{\lambda_1^w},\dots,1/\sqrt{\lambda_{\ell_w}^w}) \in \mathbb{R}^{\ell^w\times\ell^w}$, $\Phi^c = [\phi_1^c \mid \dots \mid \phi_{\ell^c}^c] \in \mathbb{R}^{(n+1)\times\ell^c}$, $\Phi^w = [\phi_1^w \mid \dots \mid \phi_{\ell^w}^w] \in \mathbb{R}^{(n+1)\times\ell^w}$, $(\mathcal{K}_c^w)_{ij} = \sqrt{\alpha_j}\sqrt{\alpha_i}\langle c^j, w^i\rangle_X, \mathcal{K}_c^w \in \mathbb{R}^{(n+1)\times(n+1)}$, $(\mathcal{K}_w^c)_{ij} = \sqrt{\alpha_j}\sqrt{\alpha_i}\langle w^j, c^i\rangle_X, \mathcal{K}_w^c \in \mathbb{R}^{(n+1)\times(n+1)}$, $(\mathcal{K}_c^c)_{ij} = \sqrt{\alpha_j}\sqrt{\alpha_i}\langle c^j, c^i\rangle_X, \mathcal{K}_c^c \in \mathbb{R}^{(n+1)\times(n+1)}$, $(\mathcal{A}_w^w)_{ij} = \sqrt{\alpha_j}\sqrt{\alpha_i}\langle \nabla w^i, \nabla w^j\rangle_X, \mathcal{A}_w^w \in \mathbb{R}^{(n+1)\times(n+1)}$, $(\mathcal{A}_c^c)_{ij} = \sqrt{\alpha_j}\sqrt{\alpha_i}\langle \nabla c^i, \nabla c^j\rangle_X, \mathcal{A}_c^c \in \mathbb{R}^{(n+1)\times(n+1)}$, $\mathcal{T}_{ij} = \sqrt{\alpha_j}\sqrt{\alpha_i}\langle v\cdot\nabla c^j, w^i\rangle_X, \mathcal{T} \in \mathbb{R}^{(n+1)\times(n+1)}$, $\mathcal{N}(\eta^c(t))_j = \langle W'(c^\ell(t)), \psi_j^c\rangle_X, \mathcal{N}(\eta^c(t)) \in \mathbb{R}^{\ell^c}$.

To handle the nonlinearity, we project the finite element solution onto the POD space for each time instance $k = 0,\dots,n$, i.e. we approximate

$$\mathcal{N}(\eta^c(t_k))_j = \langle W'(c^\ell(t_k)), \psi_j^c\rangle_{V',V} \approx \langle W'(c^k), \psi_i^c\rangle_{V',V}. \tag{13}$$

4 Numerical example

The data is chosen as follows: we consider a rectangular domain $\Omega = (0,1.5)\times(0,0.75)$, the end time $T = 0.025$, constant mobility $m \equiv 0.00002$ and a constant surface tension $\sigma = 24.5$. The interface parameter ε is set to $\varepsilon = 0.02$. As initial condition we use a circle with radius $r = 0.25$ and center $(0.375, 0.375)$. The velocity field is of parabolic type. We consider $V = H_0^1(\Omega), H = L^2(\Omega)$. By $t_j = j\Delta t$ for $0 \le j \le 1000$ with $\Delta t = 2.5\cdot 10^{-05}$ we introduce a uniform time grid. For the temporal discretization we utilize a semi-implicit Euler scheme which reads as follows: for given c^{j-1}, find c^j with associated w^j solving

$$\left\{ \begin{array}{rcll} \langle \frac{c^j - c^{j-1}}{\Delta t}, v_1\rangle_H + \langle v\cdot\nabla c^{j-1}, v_1\rangle_H + m\langle \nabla w^j, \nabla v_1\rangle_H &=& 0 & \forall v_1 \in V, \\ -\langle w^j, v_2\rangle_H + \sigma\varepsilon\langle \nabla c^j, \nabla v_2\rangle_H + \frac{\sigma}{\varepsilon}\langle W_+'(c^j) + W_-'(c^{j-1}), v_2\rangle_H &=& 0 & \forall v_2 \in V, \end{array} \right. \tag{14}$$

and $c^0 = c_0$. Note that the free energy function W is split into a convex part W_+ and a concave part W_-, such that $W = W_+ + W_-$ and W_+' is treated implicitly with respect to time and W_-' is treated explicitly with respect to time. This leads to an unconditionally energy stable time marching scheme, compare [7]. The system (14) is discretized in space utiziling piecewise linear finite elements which are spatially adapted according to the gradient jump. Snapshots of the phase field at three different time points together with the adaptive meshes are shown in figure 1.

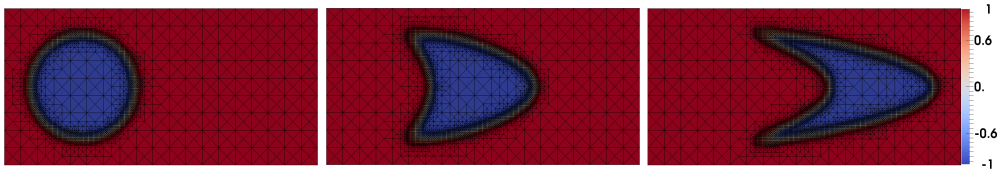

Fig. 1: *Finite element solution of the phase field c at $t = t_0, t_{500}, t_{1000}$ with adaptive meshes using W_{10000}^{rel}*

The decay of the eigenvalues of the matrix (8) for snapshots of the phase field c, the chemical potential w and the convex part of the nonlinearity $W'_+(c)$ is shown in figure 2. It shows that in the nonsmooth case with the relaxed double obstacle free energy W_s^{rel} more POD modes are needed for a good approximation than in the smooth case utilizing the polynomial free energy W^p. Table 1 summarizes the approximation quality of the solution to the POD-ROM (12) for different numbers of utilized POD modes and using different free energy functions.

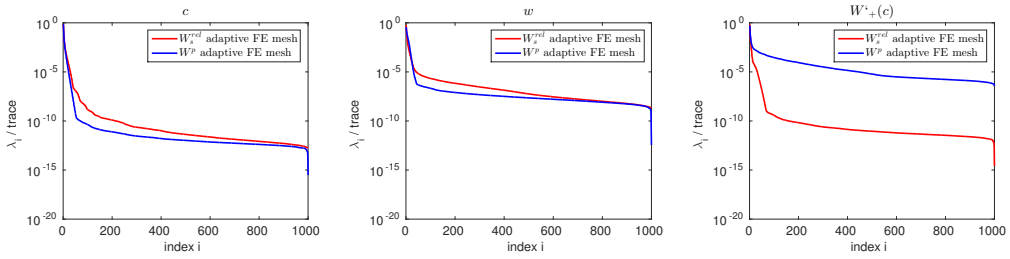

Fig. 2: *Normalized eigenvalues for c (left), w (middle), $W'_+(c)$ (right) using different free energy functions and adaptive spatial meshes*

$\ell_c = \ell_w$	ε_c, W^p	ε_w, W^p	$\varepsilon_c, W^{\text{rel}}_{10000}$	$\varepsilon_w, W^{\text{rel}}_{10000}$	ε_c, W^p, ROM-DEIM	ε_c, W^p, ROM-proj
3	$5.36 \cdot 10^{-3}$	$5.33 \cdot 10^{-2}$	$7.20 \cdot 10^{-3}$	$6.95 \cdot 10^{-1}$	$6.97 \cdot 10^{-3}$	$4.70 \cdot 10^{-2}$
5	$3.48 \cdot 10^{-3}$	$7.85 \cdot 10^{-2}$	$5.44 \cdot 10^{-3}$	$6.00 \cdot 10^{-1}$	$3.80 \cdot 10^{-3}$	$4.64 \cdot 10^{-2}$
10	$1.34 \cdot 10^{-3}$	$3.94 \cdot 10^{-2}$	$2.75 \cdot 10^{-3}$	$2.53 \cdot 10^{-1}$	$1.43 \cdot 10^{-3}$	$4.61 \cdot 10^{-2}$
20	$2.02 \cdot 10^{-4}$	$6.71 \cdot 10^{-3}$	$1.13 \cdot 10^{-3}$	$1.38 \cdot 10^{-1}$	$2.42 \cdot 10^{-4}$	$4.65 \cdot 10^{-2}$
50	$6.05 \cdot 10^{-6}$	$2.72 \cdot 10^{-4}$	$1.36 \cdot 10^{-4}$	$1.11 \cdot 10^{-2}$	$2.24 \cdot 10^{-5}$	$4.67 \cdot 10^{-2}$

Table 1: *Relative L^2-errors between the finite element and POD solution for different free energies and with DEIM and the approximation using projection, respectively*

Concerning the computational times, it turns out that the use of hyperreduction for the nonlinearity leads to an immense speedup. For the polynomial free energy, we get for $\ell_c = \ell_w = 20$ the following CPU times using adaptive meshes: finite element simulation: 1693sec, POD basis computation: 301sec, POD-ROM simulation: 160sec, POD-ROM-DEIM [6] simulation: 0.09sec, POD-ROM with projection from (13): 0.02sec. For comparison, the finite element simulation would take 8279sec on a uniform mesh with mesh size as small as the smallest triangle in the adaptive meshes.

References

[1] **H. Abels.** Diffuse Interface Models for Two-Phase flows of Viscous Incompressible Fluids. *Max-Planck Institut für Mathematik in den Naturwissenschaften, Leipzig, Lecture Note, 36, 2007.*

[2] **H. Abels, H. Garcke, G. Grün.** Thermodynamically consistent, frame indifferent diffuse interface models for incompressible two-phase flows with different densities. *Mathematical Models and Methods in Applied Sciences, 22(3):40, 2012.*

[3] **M. Ali, K. Steih, K. Urban.** Reduced basis methods based upon adaptive snapshot computations. *Advances in Computational Mathematics, 43(2):257-294, 2017.*

[4] **J. F. Blowey, C. M. Elliott.** The Cahn-Hilliard gradient theory for phase separation with non-smooth free energy. Part I: Mathematical analysis. *European Journal of Applied Mathematics, 2:233-280, 1991.*

[5] **J. W. Cahn, J. E. Hilliard.** Free energy of a non-uniform system. I. Interfacial free energy. *J. Chem. Phys. 28:258-267, 1958.*

[6] **S. Chaturantabut, D. C. Sorensen.** Nonlinear model reduction via discrete empirical interpolation. *Siam J. Sci. Comput. 32(5), 2737-2764, 2010.*

[7] **D. J. Eyre.** Unconditionally Gradient Stable Time Marching the Cahn-Hilliard Equation. *MRS Proceedings, 529, 1998.*

[8] **F. Fang, C. C. Pain, I. M. Navon, M. D. Piggott, G. J. Gorman, P. A. Allison, A. J. Goddard.** Reduced-order modelling of an adaptive mesh ocean model. *Int. J. Numer. Meth. Fluids 59: 827-851, 2009.*

[9] **C. Gräßle, M. Hinze.** POD reduced order modeling for evolution equations utilizing arbitrary finite element discretizations. *to appear in SI: Advances in Computational Mathematics, 2017.*

[10] **P. C. Hohenberg, B. I. Halperin.** Theory of dynamic critical phenomena. *Reviews of Modern Physics, 49(3):435-479, 1977.*

[11] **M. Hintermüller, M. Hinze, M. H. Tber.** An Adaptive Finite Element Moreau-Yosida-Based Solver for a Non-Smooth Cahn-Hilliard Problem. *Optim. Meth. Software 26:777-811, 2011.*

[12] **M. Hinze, J. Krenciszek, R. Pinnau.** Proper Orthogonal Decomposition for Free Boundary Value Problems. *Hamburger Beiträge zur Angewandten Mathematik, 2014.*

[13] **K. Kunisch, S. Volkwein.** Galerkin Proper Orthogonal Decomposition Methods for a General Equation in Fluid Dynamics. *SIAM J. Numer. Anal., 40(2):492-515, 2002.*

[14] **O. Lass.** Reduced order modeling and parameter identification for coupled nonlinear PDE systems. *PhD thesis, Universität Konstanz, 2014.*

[15] **L. Sirovich.** Turbulence and the dynamics of coherent structures. Parts I-II. *Quarterly of Applied Mathematics, XVL, 561-590, 1987.*

[16] **S. Ullmann, M. Rotkvic, J. Lang.** POD-Galerkin reduced-order modeling with adaptive finite element snapshots. *Journal of Computational Physics, 325:244-258, 2016.*

